



# An electrically powered gyroplane for urban air traffic

Insa Pruter<sup>1</sup> · Martin Niehuis<sup>2</sup> · Jan-Philipp Hofmann<sup>2</sup> · Holger Duda<sup>1</sup> · Armelle Zemo Mekeng<sup>1</sup> · Johannes Helbrecht<sup>1</sup> · Fabian Neumann<sup>3</sup>

Received: 12 March 2024 / Revised: 4 June 2025 / Accepted: 9 July 2025  
© The Author(s) 2025, corrected publication 2025

## Abstract

This paper aims to compare the feasibility of two different drive systems in a new electric gyroplane with two electric motors for propulsion and one electric motor for pre-rotation. The aircraft will later be used in urban and regional air traffic. Two propulsion variants are considered and investigated with regard to their flight performance and potential noise emission to examine their differences. From this, the appropriate use case for each variant could be derived. In variant 1, propulsion is provided by two large traction propellers, while variant 2 uses ducted propellers, which offer further potential for noise reduction. The static thrust for both variants has already been proven in bench tests to examine whether the two drive systems are generating sufficient thrust for an unmanned gyrocopter demonstrator with a mass of about 450 kg. Additional analytical considerations also provide initial information about the expected behavior in flight. The data obtained can help to minimize the subsequent risks in flight tests and will serve as a data base for thrust model validation to be used in the flight simulation of the gyroplane. In addition, the test data can be used to make statements about the temperature management of the drives.

**Keywords** Electric propulsion · Gyrocopters · Thrust measurements · Urban air mobility

## 1 Introduction

### 1.1 Motivation

In view of rising population growth, increased migration to metropolitan areas and growing delivery traffic, urban and inter-urban air transport will take an increasing and growing share of passenger and freight traffic. The goal of many research projects is to significantly reduce intra- and inter-urban travel times for passengers and goods. In addition, aircraft noise and environmental pollution play a decisive role in implementation [1].

The implementation of this new form of air transport requires innovative aircraft types that meet the special requirements in terms of flight performance, safety, and

noise emission. There are already numerous approaches worldwide for new aircraft configurations that address the requirements of future urban air transport, see Fig. 1.

The question of the technical feasibility with simultaneous economic efficiency of the new aircraft configurations has not yet been sufficiently answered. The DLR research project S<sup>2</sup>TOL (Silent Short Takeoff and Landing) is, therefore, investigating the technical implementation of such a concept for a quiet aircraft capable of short take-offs. In cooperation with the Institute of Jet Propulsion and Turbomachinery (IST) at RWTH Aachen University, research is being conducted on a new aircraft concept with electric propulsions for urban air transport. Special emphasis is placed on noise-optimized implementation. A significant reduction in noise emissions is expected by redesigning and arranging the propellers and rotors. In combination with the electric motor, emission-free flying is also possible. Innovative technologies such as a thrust vector control system will further optimize the short take-off capability.

### 1.2 Requirements

The noise aspect in particular plays a decisive role in the design of a new aircraft. Small aircraft operating in close

✉ Insa Pruter  
insa.pruter@dlr.de

<sup>1</sup> DLR Institute of Flight Systems, Brunswick / Aachen, Germany

<sup>2</sup> RWTH Institute of Jet Propulsion and Turbomachinery, Aachen, Germany

<sup>3</sup> DLR Institute of Lightweight Systems, Brunswick / Aachen, Germany



**Fig. 1** Future vision of urban air transport

proximity to the airport, flying slowly and at low altitude, are often perceived as disturbing. In addition to noise-reducing measures on the aircraft, a steep approach and departure should be aimed for, as noise emissions decrease sharply with altitude. Today's helicopters currently used for urban air transport operate in very small spaces, but are perceived as comparatively loud ( $> 60$  dB(A)) at low altitudes ( $< 2,000$  ft) [1].

The main reason for the high noise levels are currently common drive concepts of combustion engines in combination with propellers or rotors. As a solution, the focus is on switching to innovative propulsion concepts with a redesign of propellers and rotors to limit the noise level to 50 dB(A) at a distance of 300 m and thus meet the noise protection requirements according to Ref. [2], which defines the noise protection areas around airports with a minimum noise level at night of 50 dB(A). In combination with electric engines, there is great potential to combine emission-free and noise-optimized flying.

### 1.3 Concept study

The previously defined requirements for novel air mobility concepts are addressed by a concept study prepared by DLR. The design envisages a short take-off capable aircraft that is suitable for transporting up to four people with additional luggage for short distances (maximum take-off weight approx. 1,200 kg). The range is according to the inter-urban use case according to Ref. [3] in a purely electric variant approx. 100 km at a cruising speed of 80 kn. To increase the range to approx. 500 km and the cruising speed to 120kn/150kn, the implementation of a hybrid-electric engine is also conceivable.

While various manufacturers are focusing on configurations with tilting engines or multi-copters, the basis of these new configurations is a gyroplane. A gyroplane is a rotary-wing aircraft with a rotor driven

by the incoming air. In contrast to a helicopter, the rotor is not driven by an engine, but is in a so-called autorotation state during the entire flight. The autorotation is permanently maintained by the incoming airflow. [4]. Therefore, the gyroplane has inherent safety features that are advantageous for transport in lower airspace: For example, in the event of a malfunction, the freely rotating rotor allows for a parachute-like landing [5]. Critical flight conditions known from fixed-wing aircraft, such as stall or spin, are also not possible with gyroplanes. Due to the freely rotating rotor blades, a complex main rotor gearbox, as used in helicopters, is not necessary. This significantly reduces the manufacturing and operating costs of a gyroplane compared to a helicopter. The rotor blades are hinged to the rotor hub via a central flapping joint, so that they react to the air forces prevailing at the rotor blades with a free flapping motion [6]. In addition, the gyroplane has a pre-rotation mechanism that accelerates the rotor to take-off rotational speed before take-off.

In Europe, there is no corresponding certification regulation for gyroplanes, such as the CS-23 for light fixed-wing aircraft [7] and the CS-27 for light rotorcraft [8]. According to EU Regulation 218/1139 Annex I [9], the responsibility for gyrocopters with a maximum take-off mass of up to 600 kg lies with the national associations and authorities. In Germany, for example, today's gyroplanes are found exclusively in the class of ultralight aircraft. A type certificate is only issued according to national law and is regulated by the "Bauvorschriften für Ultraleichte Tragschrauber" (BUT) of the Luftfahrtbundesamt (German Federal Aviation Authority) [10]. This construction regulation is limited to single-engine, two-seat gyroplanes up to a maximum take-off mass of 600 kg. In UK, however, the CAA CAP 643 regulates the handling of gyrocopters [11]. However, the establishment of a uniform certification regulation for light aircraft in Europe by EASA is increasingly being discussed and is a prerequisite for further development.

For a reduced noise emission and emission-free flying, the use of different electric propulsion systems is considered. The advantages and disadvantages of these propulsion systems will be discussed later. In variant 1 of a possible design, two open propellers are used, shown in Fig. 2.

Variant 2 is designed for two ducted propellers, so-called Jetpellers from the company Jetpel GmbH,<sup>1</sup> see Fig. 3. This allows a direct comparison between the two propulsors.

The design data of the 4-seater S<sup>2</sup>TOL gyroplane from the concept study for the electric variant are shown in Table 1. The sizing of the aircraft is based on a Cessna 172 S and a R44. In addition, common two-seat gyroplanes such as the

<sup>1</sup> <https://jetpel.com/>; access date: 15.05.2025.



Fig. 2 S<sup>2</sup>TOL gyroplane variant 1 with conventional propellers



Fig. 3 S<sup>2</sup>TOL gyroplane variant 2 with ducted propellers

**Table 1** Design data of the four-seater S<sup>2</sup>TOL gyroplane for the electric variant

Max. take-off mass	approx. 1,200 kg
Payload	approx. 350 kg
Length	approx. 7 m
Span	approx. 6 m
Height	approx. 3 m
Rotor diameter	approx. 11 m
Glide ratio	5–7
Service ceiling	2000 m
Cruising speed	80 kn
Range	100 km
Take-off distance over 15 m (ISA)	< 100 m
Landing distance over 15 m (ISA)	< 100 m

MTOsport or Cavalon from AutoGyro were used for scaling. In Table 2 the mission requirements for the hybrid-electric variant are shown, too.

Compared to conventional gyroplanes, the flight performance of the configurations developed will be further optimized using new technologies to improve short take-off capability and aerodynamic adjustments to the airframe. To

**Table 2** Design data of the four-seater S<sup>2</sup>TOL gyroplane for the hybrid-electric variant

	Propeller	Jetpeller
Performance	2 × 70 kW	2 × 100 kW
Service ceiling	2500–3000 m	2500–3000 m
Cruise speed	120 kn	150 kn
Range	500 km	300 km

enable particularly short take-off and landing distances and to improve flight performance in general, the rotor of the gyroplane can be additionally powered electrically, particularly in the take-off phase but also in flight. In this way, a combination of autorotation and an actively driven rotor is achieved. The resulting yaw moment is compensated by the two engines with differential thrust. This unique new technology has already been patented [12]. To further reduce the take-off and landing distance, the implementation of tilting engines around the pitch axis is also being considered. With this type of thrust vector control, the aircraft is additionally carried by the deflected thrust during take-off.

The configuration bridges the gap between helicopter and fixed-wing aircraft. Compared to a helicopter, slightly improved flight performance as well as lower noise emissions and better efficiency are expected. Compared to a fixed-wing aircraft, significantly shorter take-off and landing distances are achieved, and the high maneuverability enables steep approaches and flying close to cities. The use for inner-city air traffic from skyscraper roof to skyscraper roof is not envisaged. The new gyroplane is a promising configuration for inter-urban air mobility. It is also suitable as a feeder from the city to the airport.

### 1.4 Goals

The aim of the project is to evaluate a new aircraft configuration in terms of flight performance, safety, and noise emission in flight tests. In addition, two different propulsion concepts with open propellers and ducted propellers are being investigated to examine their differences. From this, the appropriate use case for each variant could be derived. To be able to make statements of the flight performance and flyability of the developed aircraft, demonstrators are being built using the basic framework of an existing gyroplane. This allows a maximum take-off mass of up to 450 kg, which corresponds to a scaling of 1:3 regarding the conceptual design of the 4-seater S<sup>2</sup>TOL gyroplane (see Table 1). In a first step, it will be demonstrated that the selected engines are suitable for conducting flight tests.

## 2 Propulsion systems

The most common form of propulsion systems for small aircraft—including gyroplanes—is currently the combination of combustion engine and propeller. In the search for a more sustainable alternative, many research institutions and companies are working on the development of new propulsion systems. For short-haul aircraft, electric propulsion systems represent an alternative due to technical advances in battery technology but also the power density of electric motors and inverters in recent years [13, 14]. The concepts implemented so far rely on electrically driven propellers or rotors. In the S<sup>2</sup>TOL project, the two propulsion concepts presented in the concept study, electrically driven traction propellers and ducted propellers with hub-integrated electric motor, are being tested and compared.

### 2.1 Traction propeller

Traction propellers operate in largely undisturbed incident flow and are, therefore, most likely quieter than pusher propellers [15]. Due to their undisturbed flow, traction propellers are generally somewhat more efficient than pusher propellers but, due to their position in front of the center of gravity, they tend to have a destabilizing effect [16]. In current gyroplanes, pusher propellers are subjected to pressure fluctuations due to the arrangement behind the fuselage, the rotor mast, and the engine with a swirling turbulent inflow. In addition, the propeller area of the traction propellers can be increased more easily. A larger diameter is expected to increase efficiency by reducing the induced speeds and blade loading of the propellers, especially at low airspeeds. It is assumed that the steep climbs that can be carried out in this way after take-off offer a great advantage in terms of noise emission in the vicinity of cities.

### 2.2 Ducted propeller

Ducted propeller, as shown in Fig. 4, is a promising approach to reduce propulsion noise. This is particularly important for urban and regional air mobility.

A design with acoustically optimized blading and a large axial distance between rotor and stator, as also described in [17], contributes to reducing the propulsion noise. Due to the cut-off design, the tonal noise is not capable of propagation and is, therefore, not radiated into the far field. The tonal noise due to rotor–stator interaction is mitigated by the choice of the optimal number of blades and the large axial distance. The remaining broadband noise due to the turbulence of the inflow and wakes is directed through the covering and is low due to the use of low-loaded blades.

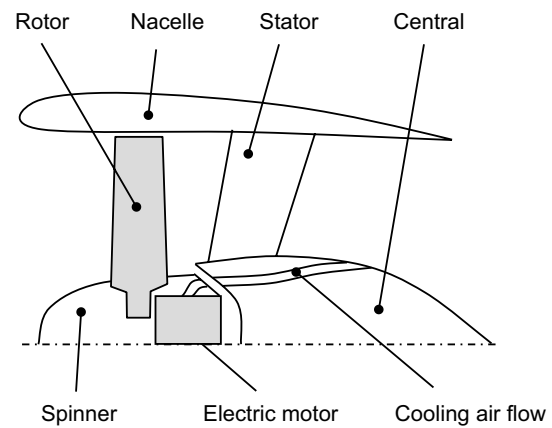


Fig. 4 Sectional view of ducted propeller

### 2.3 Comparison of the propulsion concepts

In terms of performance, the ducted propeller is characterized by increased static thrust compared to an open propeller of the same diameter. The static thrust advantage can be determined to be about 26% using momentum theory [18]. However, this thrust advantage decreases with increasing inflow velocity. As an alternative to increasing thrust, the diameter can also be reduced compared to the open propeller. With the same thrust and the same power, the necessary diameter of a ducted propeller is reduced to about 70% of the open propeller [19].

In contrast to open propellers, whose diameter can often be increased almost arbitrarily, ducted propellers are limited by the weight and the significant drag of its covering at higher speeds. Due to the smaller diameter, ducted propellers can be more easily integrated into the aircraft. In addition, the covering offers the possibility of integrating further functions such as acoustic liners or burst protection. Ground personnel and passengers are better protected.

Due to the conditioning of the flow in the inlet and the controlled jet constriction in the nozzle, the mass flow of the ducted propeller varies significantly less with the inflow speed than that of the open propeller. Thus, a wide operating range with high efficiencies is achieved even without blade pitch control. Dispensing with the pitch control mechanism reduces the complexity of the system and reduces the additional weight due to the covering.

## 3 Structure of the demonstrators

To investigate the new propulsion concepts, two demonstrators are being built and will be tested in flight. These are based on platforms from the manufacturer AutoGyro

**Table 3** Engine thrust requirements (assumption 450 kg flight mass)

Airspeed [km/h]	Required thrust [N]
0	1000
40	1000
80	875
120	675
160	535

**Table 4** Performance profile of a traffic pattern under ISA conditions (15 °C, 0 m, 1013 hPa)

Flight phase	Airspeed [km/h]	Required thrust [N]	Duration [s]
Climb	80	875	100
Cruise	120	405	500
Descent	100	200	100

GmbH with a MTOM of 450 kg. The flight testing of these demonstrators will be unmanned.

For this purpose, the demonstrators will be equipped with appropriate flight system technology. Most of this is mounted on a carrier plate in the front area of the gyroplane. The design is modular and allows the flight system technology to be exchanged between the two demonstrators. For this purpose, the entire carrier plate is replaced between the demonstrators. The on-board computer, sensors, inertial platform, and buffer battery are installed on the plate. The required actuators will be mounted at a suitable location on the gyroplane. The demonstrators are controlled by two remote pilots who control the gyroplane electronically from the ground via a pilot control station or a remote-control unit [20]. The pilots are supported by the FTL (Flight Test Lead), who is responsible for safe flight sequence.

Carrying out flight tests will provide important insights into the planned four-seater gyroplanes. Two demonstrators will be built, one of them will be equipped with open traction propellers and one with ducted propellers.

### 3.1 Requirements

Data from measurement flights carried out by DLR in 2010 were used to design the propulsion systems. These flights were conducted with a manned gyroplane of type MTOsport with 350 kg and 400 kg take-off mass [21]. Using this data, a parameter-identified simulation model was created. From this model, the thrust requirements for a gyroplane with a take-off mass of 450 kg could be derived, see Table 3.

In addition to the static thrust requirements, both types of propulsion must meet the requirements specified in Table 4.

The performance profile of a traffic pattern consists of three flight segments. For each flight segment, the requirements that must be met as a minimum have been presented in Table 4. Flight segment 1 represents the climb phase. This flight phase must be maintained for at least 100 s at an average speed of 80 km/h. The thrust requirement is at least 875 N. Flight segment 2 represents stable horizontal flight. For 500 s at 120 km/h, at least 405 N thrust shall be provided. The third flight segment describes the descent. Due to the low thrust requirements, this has no relevance in the design of the propulsion systems.

The climb rate requirements are also derived from existing measurement data and the simulation model of a manned gyroplane of the type MTOsport. For comparison, a gyroplane of the type MTOsport with a Rotax engine has a climb rate of approx. 4 m/s at a weight of 450 kg; at a take-off weight of 500 kg, the climb rate is further reduced to 3.4 m/s [22].

A limiting factor for the operation of electric propulsion systems is the overheating of the electric components. This is caused by the low permissible operating temperatures compared to conventional propulsions. When integrating these propulsion systems, the thermal management of the battery and electric motor is a major challenge. High operating temperatures lead to accelerated aging of the components. If the components reach a temperature that leads to irreversible damage, the available propulsion power or mission energy is reduced. During the entire traffic pattern, there is a requirement that the engine temperature must not rise above 95 °C and the battery temperature must not rise above 65 °C [23]. The design and construction of the two demonstrators are explained in more detail below.

### 3.2 Demonstrator#1

Demonstrator#1 with open propellers is being set up to gain initial insights into the new technologies, such as electric propulsion systems, assisted autorotation or differential thrust in flight experiments, and to derive initial assessments with regard to flight performance and noise emission, see Fig. 5.

Components from Geiger Engineering GmbH are used. This manufacturer offers a certified system consisting of motor, controller, and batteries that is already used in manned aviation. Other manufacturers in Germany could not offer this type of system, which is why only motors from Geiger Engineering GmbH were considered. The propulsion system drives the 3-blade traction propellers, which measure 1.60 m in diameter. The carbon propellers are characterized by a low pitch and a thin profile (chord@75%: 57 mm) and can be used up to 50 kW. The diameter of the

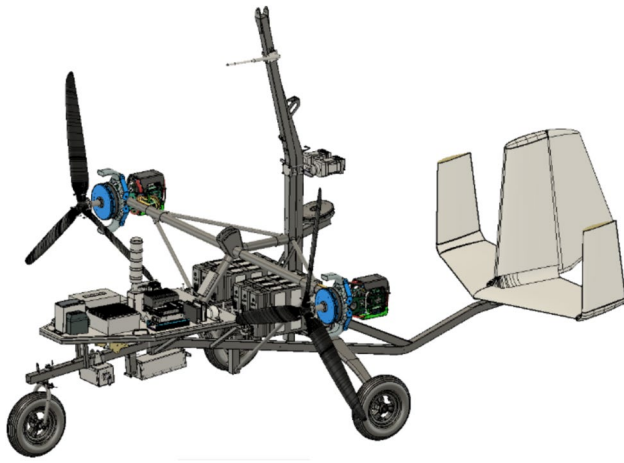


Fig. 5 Demonstrator#1 with open propellers (Source: DLR)

propeller was chosen due to the available installation space and was recommended by the motor manufacturer to achieve the required thrust from Table 3. Noise should be reduced using a propeller with a large diameter to keep the speed low and with a thin profile to reduce the drag. An engine unit consists of a permanent magnet excited synchronous motor with associated controller, which are installed on a carrier. To select a suitable motor, the thrust of the propeller was calculated analytically for different speeds using the blade element theory, considering the thrust requirements specified in Sect. 3.1. In Fig. 6, this is plotted against the mechanical power.

The required static thrust from Table 3 of 1000 N is achieved at about 20 kW mechanical power. At 40 km/h, the requirements are 25.5 kW, at 80 km/h, 120 km/h and 160 km/h about 30.5 kW. The thrust required for cruise at 120 km/h (see Fig. 6) is achieved at about 17.5 kW mechanical power.

This means that two motors from Geiger Engineering are suitable: the HPD20 motor with 20 kW continuous and 28 kW maximum power or the larger HPD32D with 32 kW continuous and 40 kW maximum power. The HPD20 motor requires a MC300 master/slave motor controller with 28 kW continuous and 40 kW maximum power. The HPD32D motor is operated together with two master/slave motor controllers with 50 kW continuous and 80 kW maximum power. The HPD32D motor weighs 11.8 kg, about twice as much as the HPD20 motor. The additional weight due to the larger controller is another 3 kg.

Assuming that the power requirement of the 1.60 m propeller matches the power of the respective electric motors, the HPD32D fully meets the power requirements according to Fig. 6. The HPD20 motor also achieves the required values in the static thrust case, but from 80 km/h airspeed, there are slight deviations of 10–15% from the

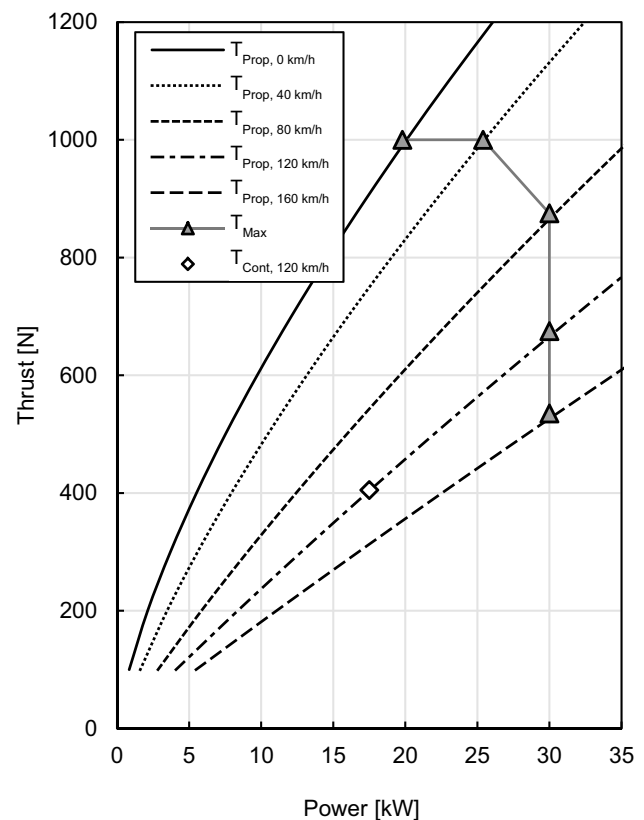


Fig. 6 Open propeller thrust  $T_{Prop}$  over mechanical power for different airspeeds as well as maximum thrust requirements  $T_{Max}$  for different speeds and continuously required thrust  $T_{Cont, 120 \text{ km/h}}$  in cruise

requirements given in Table 3. For example, at 80 km/h, a maximum of 815 N thrust is achieved; at 120 km/h a maximum of 625 N; and at 160 km/h, a maximum of 490 N thrust. Also, for these values, the assumption applies that the power requirement of the propeller is always lower than the maximum power of the electric motor, even at low speeds, so that the motor is always able to call up its maximum power. The required continuous power of approx. 17 kW can also be maintained by the HPD20.

Despite the slight limitations regarding the thrust requirements, the HPD20 motor is chosen for Demonstrator#1. The decisive factor for this decision is the higher weight of the HPD32D motor, which is due to the planned arrangement of the propulsion systems on the motor mount (see Fig. 5) would bring significant disadvantages for the design. Since the thrust requirements were originally designed for a take-off mass of 450 kg, but the take-off mass of Demonstrator#1 is expected to be only 380 kg (15% less), the deviations of the required thrust values from Table 3 are, nevertheless, within a permissible range of less than 15%.

In addition, the motor is equipped with a suitable cooling air system. The motor is cooled efficiently through targeted air supply to the coils. Using two propellers that rotate in

opposite directions, an improvement in flight behavior is expected. Thus, roll moments due to propeller drive torques as well as yaw moments due to wake on the vertical stabilizer and gyroscopic forces are reduced. To achieve minimum take-off distances with the electric demonstrators, the engines on both sides can be rotated up to  $45^\circ$  around the transverse axis during take-off and landing, so that the rotor is assisted in generating lift. The pre-rotation is carried out via an HPD 14 motor with 14 kW continuous and 18 kW maximum power. The associated MC300 controller has 12 kW continuous and 16 kW maximum power. The total energy requirement is provided by six 3.1 kWh batteries, so a total of 18.6 kWh is available. [23]. The maximum power output for three interconnected batteries is 46 kW (each for one of two drive trains), which far exceeds the demand of the HPD20 motor. In addition, a supportive drive of the main rotor is planned. The resulting yaw moment is compensated by differential thrust.

With knowledge of the calculated thrust and the estimated take-off masses, initial analytical flight performance calculations can be carried out (see Table 5).

With 4.5 m/s at 80 km/h, the gyroplane offers sufficient climb performance. The decrease in climb performance with increasing airspeed is also tolerable. The maximum flight speed is about 140 km/h.

### 3.3 Demonstrator#2

From the knowledge gained, Demonstrator#2 with two electrically driven ducted propellers is derived, see Fig. 7. The basis is a similar frame as for Demonstrator#1.

The ducted propellers to be used are being investigated at the Institute of Jet Propulsion and Turbomachinery at RWTH Aachen University in cooperation with Jetpel GmbH. The functionality of the design tools developed for this purpose as well as the design correlations determined through extensive studies are described in Ref. [24].

A design for the blades, vanes, nacelle, and nozzle of the ducted propeller originally developed for small aircraft has already been extensively tested on the static test bench at

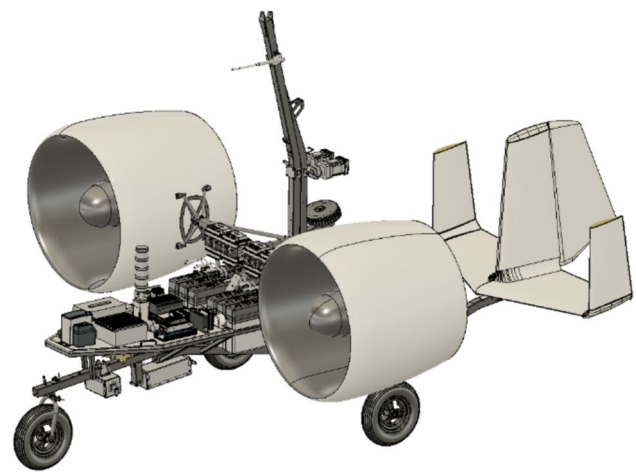


Fig. 7 Demonstrator#2 with ducted propellers (Source: DLR)

RWTH Aachen University. For the S<sup>2</sup>TOL project, it was adapted to the gyroplane application with lower power and lower flight speed.

To select a suitable motor from the manufacturer Geiger Engineering, the thrust of the propeller was calculated based on mean line flow analysis methods for different speeds [24], considering the thrust requirements specified in Sect. 3.1.

The thrust of the Jetpeller  $F_{\text{Jetpeller}}$  is shown as a function of its rotational speed for various airspeeds in Fig. 8. The map also contains the maximum thrusts from Table 3 as well as the continuously required thrust in cruise flight at 120 km/h from Table 4.

Each thrust value  $F_{\text{Jetpeller}}$  associated with a rotational speed and an inflow velocity is converted into a mechanical power  $P_{\text{Jetpeller}}$  via the characteristic diagram of the Jetpeller.

The resulting power curves over the rotational speed are shown for the same airspeeds in Fig. 9. In addition to the thrust curves, the power requirements for the maximum required thrusts and the continuously required thrust at 120 km/h are also transformed into the diagram. In addition, Fig. 9 shows the characteristic curves of the electric motor HPD40D for the maximum mechanical power  $P_{\text{HPD40D,mech,Max}}$  and the continuous mechanical power  $P_{\text{HPD40D,mech,cont}}$ . The intersections of the electric motor and Jetpeller curves indicate the operating points for continuous and peak power of the electric motor at different airspeeds.

The intersections of the characteristic curve for the maximum power of the electric motor with the characteristic curves of the Jetpeller are above the power requirements for the maximum thrust. The Jetpeller in combination with the HPD40D fulfills the requirements regarding the minimum necessary thrust from Table 3. Analogously, the intersection of the continuous power curve with the Jetpeller curves is also above the power requirement for cruising flight at

**Table 5** Climb performance and maximum flight speed of Demonstrator#1

Demonstrator#1	
Take-off mass	Approx. 380 kg
Max. electrical power	$2 \times 28 \text{ kW}$
Thrust @ 80 km/h	$2 \times 815 \text{ N}$
Thrust @ 120 km/h	$2 \times 625 \text{ N}$
Rate of climb @ 80 km/h	4.5 m/s
Rate of climb @ 120 km/h	2.8 m/s
Max. airspeed	140 km/h

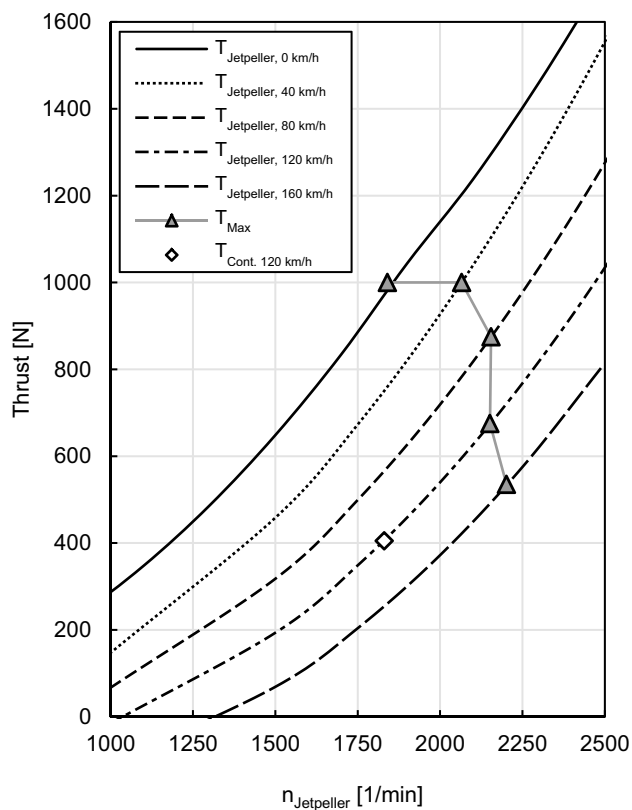


**Fig. 8** Thrust of the Jetpeller  $T_{\text{Jetpeller}}$  over its rotational speed for different airspeeds as well as maximum thrust requirements  $T_{\text{Max}}$  for different airspeeds and continuously required thrust  $T_{\text{Cont.,120 km/h}}$  in cruise flight

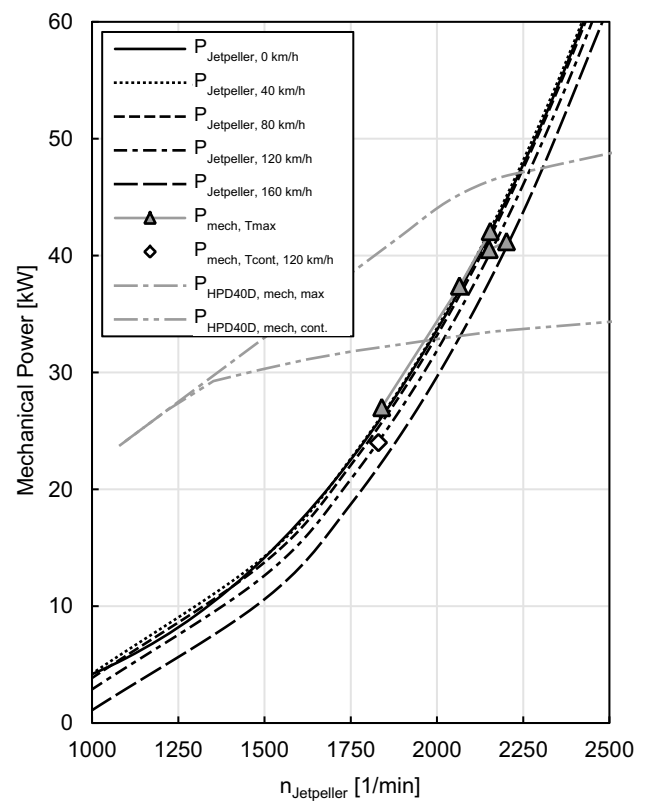


**Fig. 9** Matching of the Jetpeller and the electric motor HPD40D: power of the Jetpeller  $P_{\text{Jetpeller}}$  over its rotational speed for different airspeeds

120 km/h. Thus, the propulsion system also fulfills the requirements of the continuous operating point.

A flyable prototype of the Jetpel GmbH is shown in Fig. 10. For reasons of weight and rigidity, the Jetpellers are predominantly of integral construction made of carbon fiber.

To operate the hub-integrated HPD40D, two MC300 master/slave motor controllers each with 50 kW continuous and 80 kW maximum power are required. These are attached directly to the frame of the gyroplane near the batteries. A cooling air system is integrated into the hub to cool the motors.

The Jetpeller Prototype was designed at the Institute for Jet Propulsion and Turbomachinery [24]. The data from the pre-design have already been validated with CFD data. The same system as for Demonstrator#1 is used for the pre-rotation. In contrast to Demonstrator#1, the total energy demand is provided by 12 1.55 kWh batteries, so a total of 18.6 kWh is available as in Demonstrator#1 [23]. The total weight of the batteries is comparable to that of the batteries of Demonstrator#1. The difference is related to the controllers used. Due to the duplex system, the controllers—two per Jetpeller—must be powered separately.



**Fig. 10** Jetpeller for Demonstrator#2 (Source: DLR)

Using three batteries per side, as in Demonstrator#1, would result in an asymmetrical distribution, which leads to a heavier load on the individually used battery. Switching to the smaller batteries allows a symmetrical distribution, so that each controller unit is powered by three batteries. The

six batteries used per Jetpeller have a combined maximum power output of 49 kW. With knowledge of the calculated thrust and the estimated take-off masses, the resulting flight performance is shown in Table 6.

Demonstrator#2 reaches a maximum flight speed of 160 km/h. The climb performance meets all requirements in the low speed range with 4.0 m/s. Even in the higher speed range, with 2.9 m/s, there is still enough climb performance.

### 3.4 Comparison of the demonstrators

The demonstrators differ in weight and performance due to their different propulsion systems. The values are shown in Table 7.

Demonstrator#2 is altogether about 50 kg heavier than Demonstrator#1. This is partly due to the more powerful and redundant electric engine system. The motors of Demonstrator#2 have an additional weight of about 13 kg, the associated controllers weigh about 7 kg more. In return, Demonstrator#2 also has twice the power available with 2\*60 kW vs. 2\*28 kW. However, due to the limited power output of the batteries, only 49 kW of this can be used per propulsion. Furthermore, the additional weight is due to the use of the ducted propellers instead of the open propellers. The Jetpeller prototypes weight about 30 kg more than the propulsion unit of the open propeller without the electrical components. One advantage of Demonstrator#2 is the significantly smaller rotor diameter, which allows for a more compact design. The choice of the diameter of the ducted propeller is primarily determined by cruise flight to keep the energy consumption low. In general, a smaller diameter reduces the nacelle drag in cruise flight and, in return, requires a high take-off power. This power requirement can be met by the high, but time-limited, peak power of the electric motor, and thus a small diameter can be realized for high overall efficiency in cruise flight.

**Table 6** Flight performance of Demonstrator#2

Demonstrator#2	
Take-off mass	Approx. 430 kg
Max. electrical power	2×49 kW
Thrust @80 km/h	2×875 N
Thrust @120 km/h	2×675 N
Rate of climb @80 km/h	4.0 m/s
Rate of climb @120 km/h	3.0 m/s
Max. airspeed	Approx. 160 km/h

**Table 7** Technical data of both demonstrators

	Dem#1	Dem#2
Take-off mass	Approx. 380 kg	Approx. 430 kg
Motor	HPD20	HPD40
Maximum power (electr.)	2×28 kW	2×60 kW
Continuous power (electr.)	2×20 kW	2×40 kW
Battery capacity	18.6 kWh	18.6 kWh
Max. power output batteries	2×46 kW	2×49 kW
Propeller/rotor diameter	1,60 m	0,85 m

## 4 First test results

The testing of the demonstrators enables an experimental comparison of the two propulsion systems presented. The evaluation is carried out with regard to thrust, power, and noise. Initial test bench results provide static thrust for various powers and allow a comparison with the analytical calculation from chapter 3.

### 4.1 Demonstrator#1

The open 1.6 m propeller from the company E-Props was tested with a motor unit on the thrust measurement test bench of the Institute for Jet Propulsion and Turbomachinery. On this test bench, static thrust measurements were carried out at various propeller speeds and the performance profile of a traffic pattern specified in the requirements was simulated.

The static thrust curve from Sect. 3.2 supplemented by the measured values is shown in Fig. 11.

For the four speeds and power levels, the measured thrust agrees sufficiently well with the previously calculated thrust.

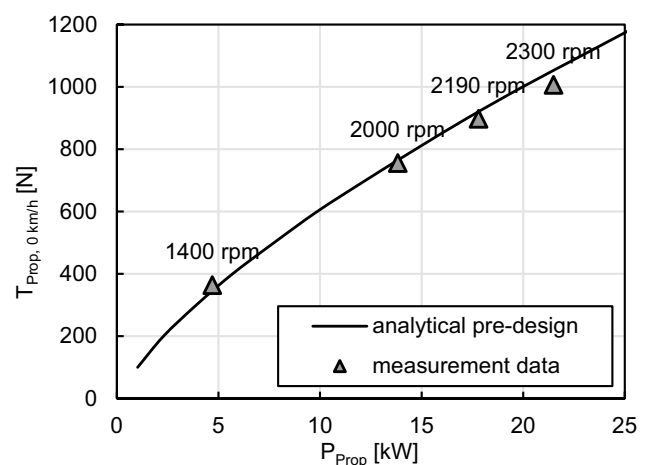


**Fig. 11** Thrust of the open propeller  $F_{Prop, 0 km/h}$  via mechanical power  $P_{Prop}$ , comparison of the data from the analytical prediction and the measured data from the bench tests

At higher power levels, the accuracy decreases. Reasons for this discrepancy could be attributed to motor losses due to increased friction resulting from the physical contact by rotating components within the motor at higher rpm [25]. Furthermore, general viscous losses could lead to a poorer match. This could lead to a reduced thrust. However, the required maximum static thrust of 1000 N is achieved. Therefore, it is assumed that the thrust curves of different speeds also represent the characteristics of the propeller well.

Figure 12 also shows the results from the bench tests for Demonstrator#1 for the completed performance profile according to Table 4. For this, rotational speeds were set at which the retrieved torque of the electric motor roughly corresponds to that of the specified flight condition. The power was supplied via only two instead of the three batteries planned later.

The required performance according to Table 3 and Table 4 is achieved. It should be noted that the measured values correspond to the static thrust, which is why they are higher than in the actual flight phase. The increase in battery temperature is to be regarded as critical. In the test carried out, Sect. 2 (traffic pattern) of the specified performance profile had to be aborted after approx. 380 s to prevent

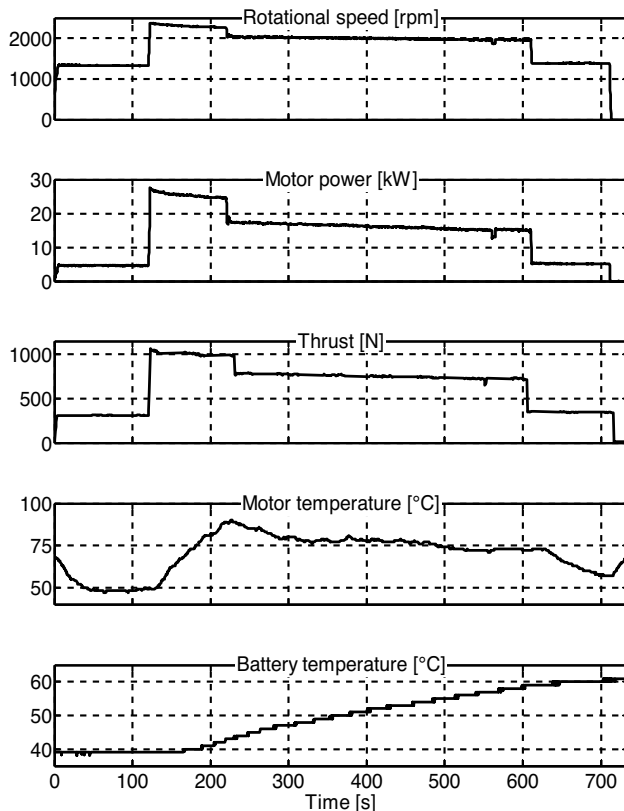


**Fig. 12** Tested performance profile for the open propellers in the test rig

damage to the batteries due to an excessively high operating temperature. Since the bench tests were only carried out with two batteries, it is assumed that the planned use of three batteries in the flight test will reduce the temperature of the batteries and thus the required 500 s (Table 4, performance profile of a traffic pattern) can be achieved. In addition, the initial temperature with almost 40 °C was relatively high. The flight time could be further increased by keeping the initial temperature of the batteries as low as possible before the start of the flight. This could be achieved by active cooling before and during the flight.

A cooling air system allows the motor temperature to be kept at a maximum of 89 °C even after phases of maximum load. To prevent accelerated aging, the limit temperature of the electric motor is 95 °C. The motor cools down again in phases of lower load.

## 4.2 Demonstrator#2

The analytical calculations and the measurements of the static thrust of the Jetpeller are shown in Fig. 13. The static thrusts measured by the IST in the bench tests agree sufficiently well with the prediction according to [24] and thus fulfill the requirements of Table 3 in the static position. It is, therefore, assumed that the thrust curves for higher speeds also represent the characteristics of the Jetpeller well.

The results from the bench tests of the Jetpeller for the performance profile according to Table 4 are shown in Fig. 14.

The tests were carried out with four 3.1 kWh batteries instead of the smaller 1.55 kWh batteries, as these were not yet available at the time of the tests. Four batteries were chosen to ensure symmetrical distribution among the controllers.

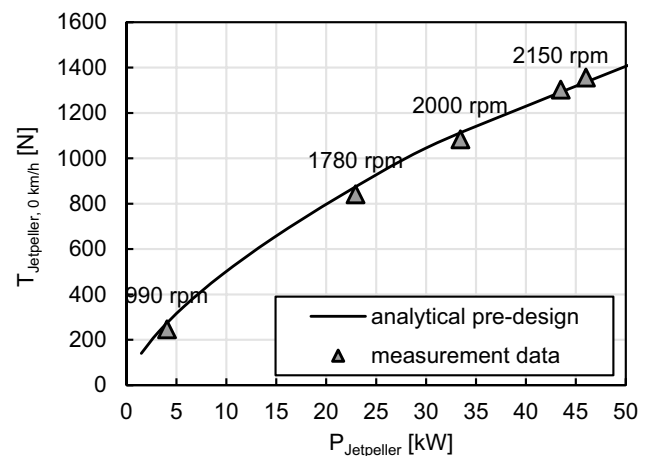


**Fig. 13** Thrust of the Jetpeller  $T_{\text{Jetpeller}, 0 \text{ km/h}}$  via mechanical power  $P_{\text{Jetpeller}}$ , comparison of the data from the analytical prediction and the measured data from the bench tests

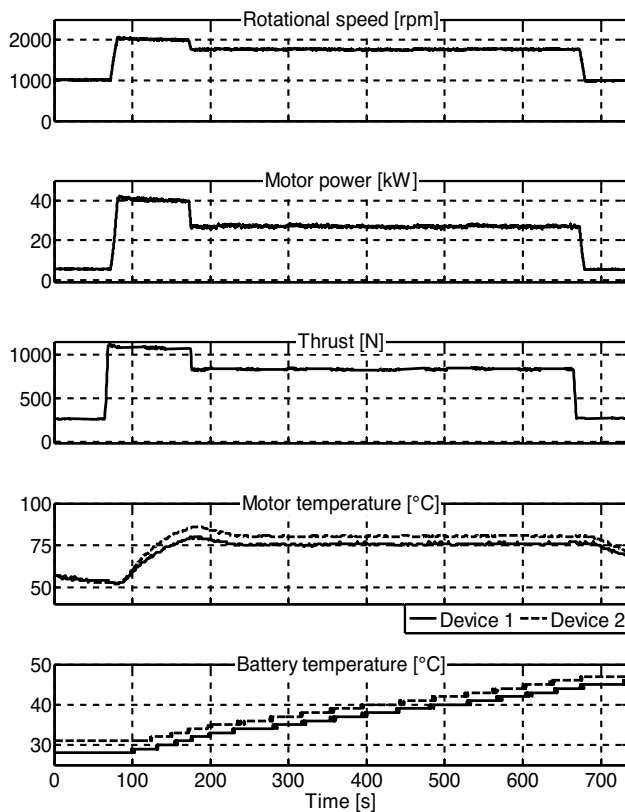


Fig. 14 Tested performance profile for the Jetpeller in the test rig

The Jetpeller Prototype was already able to fully meet the required performance profile of a traffic pattern. As with the motor unit of the open propeller, the motor temperature rises significantly when maximum thrust is called up for a longer period of time. Within the specified 100 s, the temperature of 80/83 °C is still well below the critical temperature of 95 °C. It is also noticeable in this test run that with the selected performance profile, the battery temperatures and not the capacity of the batteries could limit the operating time.

## 5 Conclusion and outlook

This paper describes the concept and construction of two electrically powered gyroplane configurations for urban air traffic. The two types of propulsion systems, open propellers and ducted propellers, so-called Jetpellers, are considered and compared with each other with regard to their characteristics and flight performance. The configurations will be tested with unmanned demonstrators with a take-off mass of up to 450 kg.



Fig. 15 Demonstrator#1 with electrically driven propellers (380 kg MTOM)

## 5.1 Results

Based on the results from the bench tests, it can be stated that the thrust values calculated analytically in chapter 3 are valid. Overheating of the motors or the controllers on the given traffic pattern is unlikely, but the temperature of the batteries must be monitored and an effective warning system must be integrated. If necessary, further cooling measures must be taken.

For Demonstrator#1 with open propellers, the required static thrust was proven by bench tests. This fits very well with the analytical thrust model. The performance profile of a standard traffic pattern was also successfully completed in the test rig. Initial flight performance calculations show that the required rate of climb is achieved for low airspeeds. For higher airspeeds, the climb rate is slightly reduced. The maximum flight speed is 140 km/h.

Demonstrator#2 with the Jetpellers also meets the requirements for static thrust in the test rig. The performance profile of a standard traffic pattern was also successfully completed in the bench tests. The required climb rates are achieved. The maximum airspeed is 160 km/h. The analytically calculated flight performance data must be verified in further tests.

Using open propellers, a lighter and simpler design can be implemented. As a result, the power requirement is lower. This allows a greater range. The ducted propellers, on the other hand, are more powerful, which enables faster flying. Another advantage is their more compact design.

## 5.2 Outlook

In the next step, the propulsion systems will be further tested with mobile bench tests. For this purpose, thrust measurements of both propulsion systems will be carried out under

variable incident flow velocities and angles. The variation of the inflow speed is made possible by mounting the tests rig on a vehicle. Flight testing will be carried out in June 2025—first with Demonstrator#1 (see Fig. 15), later with Demonstrator#2.

As part of a virtual flight test, both demonstrators will be flown in the DLR flight simulator. Together with experienced gyroplane pilots, the flyability and flight performance will be tested and evaluated. The findings from these simulator studies will be incorporated into further testing and construction of the demonstrators. First flights in the simulator with Demonstrator#1 already show promising results.

After successful testing of the demonstrators, a prototype for the four-seater version from the concept study is conceivable for marketing. The noise-optimized propulsion systems in combination with the excellent flight characteristics and low acquisition and maintenance costs of the gyroplane offer great potential to place this configuration sustainably on the advanced air mobility market. Applications for passenger transport or cargo drone appear attractive.

**Author contribution** I.P. and M.N. write the main manuscript text. J.-P.H. played a key role in writing the chapter “Propulsion System” and supported the evaluation of the bench tests. H.D. contributed to the evaluation of the flight performance. A.Z.M. prepared Figs. 5, 7, 12, and 14 and supported the evaluation. J.H. took part in the concept study and F.N. contributed the paragraphs to EASA certification. All authors reviewed the manuscript.

**Funding** Open Access funding enabled and organized by Projekt DEAL.

**Data availability** No datasets were generated or analyzed during the current study.

## Declarations

**Conflict of interests** The authors declare no competing interests.

**Open Access** This article is licensed under a Creative Commons Attribution 4.0 International License, which permits use, sharing, adaptation, distribution and reproduction in any medium or format, as long as you give appropriate credit to the original author(s) and the source, provide a link to the Creative Commons licence, and indicate if changes were made. The images or other third party material in this article are included in the article's Creative Commons licence, unless indicated otherwise in a credit line to the material. If material is not included in the article's Creative Commons licence and your intended use is not permitted by statutory regulation or exceeds the permitted use, you will need to obtain permission directly from the copyright holder. To view a copy of this licence, visit <http://creativecommons.org/licenses/by/4.0/>.

## References

1. Holden, J., Nikhil, G. (2016), *Fast-Forwarding to a Future of On-Demand Urban Air Transportation*, Uber Elevate
2. Bundesministerium der Justiz: Gesetz zum Schutz gegen Fluglärm, 2007
3. Asmer, L. (2021), *Urban Air Mobility Use Cases and Technology Scenarios for the HorizonUAM Project*, Urban Air Mobility Virtual Symposium, 22–23 September 2021, virtual.
4. Duda, H., Seewald, J.: *Flugphysik der Tragschrauber - Verstehen und Berechnen*, ISBN 978-3-662-52833-4. Springer Vieweg, Germany (2016)
5. JARUS: JARUS guidelines on Specific Operations Risk Assessment (SORA), Joint Authorities for Rulemaking of Unmanned Systems, JAR-DEL-WG6-D.04, 2017
6. Bittner, W.: *Flugmechanik der Hubschrauber*, ISBN 978-3-642-54286-2. Springer-Verlag, Berlin Heidelberg New York, Germany (2002)
7. EASA: CS-23 Normal, Utility, Aerobatic and Commuter Aeroplanes, CS-23 Amendment 6 and AMC & GM to CS-23 Issue4, 2023
8. EASA: CS-27 Amendment 9, 2021
9. EU Regulation (EC) 2018/1139, 2024 (OJ L 212 22.8.2018, p.1) <http://data.europa.eu/eli/reg/2018/1139/2024-12-01>
10. DFS Deutsche Flugsicherung: *Bekanntmachung von Bauvorschriften für Ultraleichte Tragschrauber (einmotorig)*, 2019
11. CAA: CAP 643, *British Civil Airworthiness Requirements, Section T Light Gyroplanes*, 2013
12. Duda, H., Seewald, J., Sachs, F., Lorenz, S.: *Offenlegungsschrift DE 10 2020 134 686 A1 2022.06.23*, Deutsches Patent- und Markenamt, 2022
13. Viswanathan, V., Knapp, B.M.: Potential for electric aircraft. *Nat. Sustain.* **2**, 88–89 (2019), <https://doi.org/10.1038/s41893-019-0233-2>
14. Schäfer, A.W., Barrett, S.R.H., Doyme, K., et al.: Technological, economic and environmental prospects of all-electric aircraft. *Nat. Energy* **4**, 160–166 (2019), <https://doi.org/10.1038/s41560-018-0294-x>
15. Schuller, J.B.H.M.: Analysis of the excess noise of aircraft pusher propellers. *J. Acoust. Soc. Am.* **105**, 1184 (1990), <https://doi.org/10.1121/1.425590>
16. Roskam, J.: *Airplane Design Part II: Preliminary Configuration Design and Integration of the Propulsion System*, DARcorporation, ISBN-13: 978-1884885433, 2017
17. Koppelberg, J., Weintraub, D., Jeschke, P.: Acoustic pre-design studies of ducted fans for small aircraft. *CEAS Aeronaut. J.* **13**, 877–889 (2022), <https://doi.org/10.1007/s13272-022-00604-3>
18. Black, D.M., Wainauski, H.S., Rohrbach, *Shrouded Propellers – A Comprehensive Performance Study*, AIAA, No. 68–994, Philadelphia, Pennsylvania, 1968
19. Jeschke, P.: *Manuskript zur Vorlesung Luftfahrtantriebe I und II*, Institut für Strahlantriebe und Turbomaschinen RWTH Aachen, 2023
20. Laubner, M., Bender, S., Goormann, L., Lorenz, S., Pruter, I., Rudolph, M.: *A Remote Test Pilot Control Station for Unmanned Research Aircraft*, DLRK 2022, Dresden
21. Pruter, I., Duda, H.: *Flugversuche zur Systemidentifizierung eines MTOsports im Projekt GyroTrain*, Institutsbericht IB 111–2010/57, DLR Braunschweig, 2010
22. *AutoGyro - Flight and Operation Manual for Gyrocopters MTOsport*, 2016
23. Geiger, J.: *Handbuch Elektrisches Antriebssystem komplett*, Geiger Engineering, 2021

24. Weintraub, D., Koppelberg, J., Köhler, J., Jeschke, P.: Ducted fans for hybrid electric propulsion of small aircraft. *CEAS Aeronaut. J.* **13**, 471–485 (2022), <https://doi.org/10.1007/s13272-022-00573-7>
25. Roshandel, E., Mahmoudi, A., Kahourzade, S., Yazdani, A., Shafiullah, G.: Losses in efficiency maps of electric vehicles: an overview. *Energies* (2021), <https://doi.org/10.3390/en14227805>

**Publisher's Note** Springer Nature remains neutral with regard to jurisdictional claims in published maps and institutional affiliations.